MITSUBISHI ELECTRIC RESEARCH LABORATORIES
http://www.merl.com

Robust Nonlinear State Estimation for Thermal-Fluid Models Using Reduced-Order Models: The Case of the Boussinesq Equations

Benosman, M.; Borggaard, J.

TR2019-147 December 11, 2019

Abstract

We present a method for designing robust, proper orthogonal decomposition (POD)-based, low-order observers for a class of spectral infinite-dimensional nonlinear systems. Robustness to bounded model uncertainties is incorporated using the Lyapunov reconstruction approach from robust control theory. Furthermore, the proposed methodology includes a data-driven learning algorithm that auto-tunes the observer gains to optimize the performance of the state estimation. A challenging numerical example using the 2D Boussinesq equations demonstrates the effectiveness of the proposed observer.

IEEE Conference on Decision and Control (CDC)

This work may not be copied or reproduced in whole or in part for any commercial purpose. Permission to copy in whole or in part without payment of fee is granted for nonprofit educational and research purposes provided that all such whole or partial copies include the following: a notice that such copying is by permission of Mitsubishi Electric Research Laboratories, Inc.; an acknowledgment of the authors and individual contributions to the work; and all applicable portions of the copyright notice. Copying, reproduction, or republishing for any other purpose shall require a license with payment of fee to Mitsubishi Electric Research Laboratories, Inc. All rights reserved.

Copyright © Mitsubishi Electric Research Laboratories, Inc., 2019
201 Broadway, Cambridge, Massachusetts 02139

Robust Nonlinear State Estimation for Thermal-Fluid Models Using Reduced-Order Models: The Case of the Boussinesq Equations

Mouhacine Benosman, Jeff Borggaard

Abstract— **We present a method for designing robust, proper orthogonal decomposition (POD)-based, low-order observers for a class of spectral infinite-dimensional nonlinear systems. Robustness to bounded model uncertainties is incorporated using the Lyapunov reconstruction approach from robust control theory. Furthermore, the proposed methodology includes a data-driven learning algorithm that auto-tunes the observer gains to optimize the performance of the state estimation. A challenging numerical example using the 2D Boussinesq equations demonstrates the effectiveness of the proposed observer.**

I. INTRODUCTION

One of the important problems in heating, ventilation, and air conditioning (HVAC) management is to estimate the entire spatial profile of the airflow and temperature under a limited number of sensors, placed at some optimal locations in a room. However due to the complexity of the partial differential equations (PDEs) that model indoor airflow and temperature, this estimation problem is challenging. Two well known PDE models of such systems are the Navier Stokes (NS) equations for airflow, and the Boussinesq equations for the coupled airflow and temperature model. Several observers have been proposed for the NS equation, e.g., [8], [12], [21]. For the Boussinesq equation far fewer estimation results are available due to the challenging coupling nonlinearity between the NS equation and the thermal equation. Furthermore, this estimation problem is rendered even more complex when one considers model uncertainties, which are ubiquitous in real-life applications. Indeed, there are many works that utilize adaptive control to design observers for uncertain PDE systems, where both system states and parametric uncertainties are estimated, see e.g., [19] and references therein. However, due to the complexity of simultaneously estimating both the states and model parameters, the results are often limited to linear or semi-linear PDEs with linear parametric uncertainty.

Fewer works consider robust control to design observers for PDEs in the presence of parametric model uncertainties and/or measurement noise. However, in the recent work [18], one-dimensional, semi-linear PDEs are considered and the assumption of a sector nonlinearity allows the use of dissipativity to design observers that are robust to spill-over effects. In [5], the authors consider the case of a PDE with a quadratic nonlinearity where the states and measurements are subject to time-varying disturbances. A MinMax approach was used to design a stabilizing robust observer/controller, based on the tangent linearization of the PDE along a steady state solution. Then model reduction was carried out following two approaches. In one approach, an H_2-model reduction was used for the linearized system. In the second, a proper orthogonal decomposition (POD) model reduction method for nonlinear systems was used to reduce the extended Kalman filter as in [1]. In [14], the authors propose an interval state estimator for a class of uncertain parabolic PDE systems, under homogeneous Dirichlet boundary conditions, based on a finite-element approximation of a PDE. In [17], a robust observer based on a super twisting algorithm, which ensures finite-time convergence, is introduced for a class of hyperbolic PDEs with bounded additive perturbations. In [7], the authors study the problem of stabilization and observer design for the heat equation under uncertain boundary conditions. They propose a two-stage unknown input observer to estimate the uncertainty term and then observe the system states.

In this paper, we propose a methodology to design a robust observer for a class of spectral infinite-dimensional nonlinear systems that use a low-dimensional subspace, such as POD in the observer design. The observer is based on Lyapunov reconstruction theory to 'dominate' the influence of parametric uncertainties. Furthermore, we extend this methodology so that it will auto-tune the observer gains online, using data-driven optimization methods.

In the sequel, we begin by introducing some basic definitions and notation in Section II. Section III is dedicated to introducing the class of nonlinear PDEs studied here, and presents the nominal observer design for a special class of nonlinearities. We use Section IV to introduce the first result of the paper, which is the robustification of the observer under bounded model uncertainties. The second result of the paper is presented in Section V, where we introduce the iterative feedback tuning (IFT) version of the robust observer. Section VI is used to present the third result which is the application of the proposed robust observer and its IFT extension to the 2D Boussinesq equations. We conclude the paper commenting on potential future developments of this work in Section VII.

II. BASIC NOTATION AND DEFINITIONS

For a vector $q \in \mathbb{R}^n$, its transpose is denoted by q^T, for a matrix $C \in \mathbb{R}^{n\times m}$, the transpose is denoted by C^*. The Euclidean vector norm for $q \in \mathbb{R}^n$ is denoted by $\|\cdot\|$ so that $\|q\|_{\mathbb{R}^n} = \|q\| = \sqrt{q^T q}$. The Kronecker delta function is defined as: $\delta_{ij} = 0$, for $i \neq j$ and $\delta_{ii} = 1$. We shall abbreviate the time derivative by $\dot{f}(t,x) = \frac{\partial}{\partial t} f(t,x)$, and consider the following Hilbert space $\mathcal{H} = L^2(\Omega)$. We define the inner product $\langle\cdot,\cdot\rangle_{\mathcal{H}}$ and the associated norm $\|\cdot\|_{\mathcal{H}}$ on $\mathcal{H}$ as $\langle f, g\rangle_{\mathcal{H}} = \int_\Omega f(x)g(x)dx$, for $f, g \in \mathcal{H}$, and $\|f\|^2_{\mathcal{H}} =$

$\int_\Omega |f(x)|^2 dx$. A function $z(t,x)$ is in $L^2([0,t_f];\mathcal{H})$ if for each $0 \le t \le t_f$, $z(t,\cdot) \in \mathcal{H}$, and $\int_0^{t_f} \|z(t,\cdot)\|_{\mathcal{H}}^2 dt < \infty$. We will use the standard notation from distributed parameter control theory and drop the "$\cdot$" when it is understood, e.g., $z(t) = z(t,\cdot) \in \mathcal{H}$. A pseudo-inverse of an operator $\mathcal{T}$ on $\mathcal{H}$ will be denoted as $\mathcal{T}^\dagger$, and its adjoint operator on $\mathcal{H}$ is denoted by $\mathcal{T}^*$. In the sequel when we discuss the boundedness of a solution for an impulsive dynamical system, we mean uniform boundedness as defined in [9] (p. 67, Definition 2.12). Finally, an impulsive dynamical system is said to be well-posed, if it has well-defined distinct resetting times, admits a unique solution over a finite forward time interval, and does not exhibit any Zeno solutions, i.e., does not have an infinite number of resettings in the system over any finite time interval [9].

III. PROBLEM STATEMENT AND OBSERVER DESIGN

We consider the state estimation problem for nonlinear systems of the form

$$\begin{aligned} \dot{z}(t) &= Az(t) + Bu(t) + h(z(t), u(t)), \quad z(0) = z_0, \\ y(t) &= Cz(t), \end{aligned} \tag{1}$$

where $z_0 \in D(A) \subset \mathcal{H}$, A is a linear operator that generates a C_0-semigroup on the Hilbert space $\mathcal{H}$, $B : \mathbb{R}^m \to \mathcal{H}$ is an input operator, $C : D(A) \to \mathbb{R}^p$ is the bounded linear operator for measurements, and h contains higher-order terms. For the well posedness of the estimation problem, we assume that system (1) satisfies the following assumption.

Assumption 1: The Cauchy problem for equation (1) has a solution with bounded norm $\|.\|_{\mathcal{H}}$ for any initial condition $z_0 \in D(A)$.

Furthermore, for analysis purposes we assume that h satisfies the Lipschitz assumption:

Assumption 2: The function $h : D(A) \times \mathbb{R}^m \to [D(A)]'$ satisfies $h(0,0) = 0$ and the local Lipschitz assumption: for every pair $(z,u) \in D(A) \times \mathbb{R}^m$, there exist positive constants ϵ_z, ϵ_u, L_z, and L_u such that

$$\|h(z,u) - h(\tilde{z},\tilde{u})\|_{\mathcal{H}} \le L_z \|z - \tilde{z}\|_{\mathcal{H}} + L_u \|u - \tilde{u}\|_{\mathbb{R}^m},$$

for all $(\tilde{z},\tilde{u}) \in D(A) \times \mathbb{R}^m$ satisfying

$$\|z - \tilde{z}\|_{\mathcal{H}} < \epsilon_z \qquad \text{and} \qquad \|u - \tilde{u}\|_{\mathbb{R}^m} < \epsilon_u.$$

We define a low-dimensional subspace $\hat{\mathcal{H}} \subset \mathcal{H}$ that inherits the norm of $\mathcal{H}$, i.e., $\|\cdot\|_{\hat{\mathcal{H}}} = \|\cdot\|_{\mathcal{H}}$, and follow the framework in e.g. [2] in designing the nominal observer, while changing the roles for some operators. Consider an observer with the following structure

$$\dot{\hat{z}} = A_c \hat{z}(t) + B_c u(t) + Fy(t) + G(\hat{z}(t), u(t)), \tag{2}$$

with $\hat{z}(0) = \hat{z}_0 \in D(A_c)$, and where $A_c : \hat{\mathcal{H}} \to \hat{\mathcal{H}}$, $B_c : \mathbb{R}^m \to \hat{\mathcal{H}}$, $F : \mathbb{R}^p \to \hat{\mathcal{H}}$, and $G : \hat{\mathcal{H}} \times \mathbb{R}^m \to \hat{\mathcal{H}}$ are to be determined. Possible choices for $\hat{\mathcal{H}}$ may be the space spanned by a set of dominant eigenfunctions of A (modal approximation) or a set of basis functions obtained by performing a proper orthogonal decomposition (POD) of a collection of simulations of (1) and truncating (POD approximation).

Let $\mathcal{T} : \mathcal{H} \to \hat{\mathcal{H}}$ be the orthogonal projector from $\mathcal{H}$ to $\hat{\mathcal{H}}$ (hence, $\|\mathcal{T}\|_{\mathcal{H}} = 1$) and $\mathcal{T}^\dagger$ be the injection from $\hat{\mathcal{H}}$ into $\mathcal{H}$: $\mathcal{T}^\dagger \hat{z} = \hat{z}$ for all $\hat{z} \in \hat{\mathcal{H}} \subset \mathcal{H}$. Then we define the *reduced estimation error* as

$$e(t) = \hat{z}(t) - \mathcal{T}z(t) \in \hat{\mathcal{H}}. \tag{3}$$

This can be used as a proxy for the *state estimation error*, $e_{\text{se}} \equiv \mathcal{T}^\dagger \hat{z} - z \in \mathcal{H}$, when $\mathcal{T}$ produces a small projection error $(z - \mathcal{T}^\dagger \mathcal{T} z)$, since $e_{\text{se}}(t) = \mathcal{T}^\dagger e(t) - \big(z(t) - \mathcal{T}^\dagger \mathcal{T} z(t)\big)$. When $\hat{\mathcal{H}}$ is the span of r dominant POD basis functions and $\mathcal{T}_{\text{POD}}$ is the corresponding projection for a specific trajectory z, then $\mathcal{T}_{\text{POD}}$ minimizes the projection error

$$\mathcal{P}(\mathcal{T}, z) = \left(\int_0^{t_f} \|z(t) - \mathcal{T}^\dagger \mathcal{T} z(t)\|_{\mathcal{H}}^2 \, dt \right)^{1/2}, \tag{4}$$

over all projections $\mathcal{T}$ into subspaces of $\mathcal{H}$ with dimension r, and where t_f denotes the finite time support over which the projection error is evaluated, cf. [11]. Although we are free to choose B_c and G in the observer (2), to guarantee convergence we shall make the following natural assumptions for the remainder of this paper

$$B_c = \mathcal{T}B \qquad \text{and} \qquad G(\hat{z}, u) = \mathcal{T}h(\mathcal{T}^\dagger \hat{z}, u) \tag{5}$$

for all $\hat{z} \in \hat{\mathcal{H}}$ and $u \in \mathbb{R}^m$.

We can now state our first result.

Theorem 1: Consider the system described by (1) under Assumptions 1, 2, for which we associate the state observer defined by (2) and (5). We assume that F, A_c, and $\mathcal{T}$ satisfy the conditions

$$[A_c \mathcal{T} - \mathcal{T} A + FC]\, z = 0, \qquad \text{for all } z \in D(A), \tag{D0}$$

$$\|e^{A_c t}\|_{\hat{\mathcal{H}}} \le M e^{-\delta t}, \qquad \text{for all } t > 0 \tag{D1}$$

and,

$$\delta > M L_z, \tag{D2}$$

where $M \ge 1$ and $\delta > 0$. Then we can guarantee the exponential stability of the estimation error, $e(t)$ in (3). Namely, there exists a constant c, depending on δ, M, the initial error $\|e(0)\|_{\hat{\mathcal{H}}}$, and the $\mathcal{P}(\mathcal{T}, z)$ in (4) such that

$$\|e(t)\|_{\hat{\mathcal{H}}} \le c e^{(M L_z - \delta)t} \|e(0)\|_{\hat{\mathcal{H}}}, \tag{6}$$

where,

$$c = M \left\{ \|e(0)\|_{\hat{\mathcal{H}}} + L_z \left(\frac{e^{2\delta t_f} - 1}{2\delta} \right)^{\frac{1}{2}} \mathcal{P}(\mathcal{T}, z) \right\}. \tag{7}$$

Proof 1: Refer to [4].

A. Observer Design Based on the Proper Orthogonal Decomposition

We first compute the proper orthogonal decomposition (POD) from solutions to (1) then use this as a basis for $\hat{\mathcal{H}}$. Since POD and Galerkin projection is a well-known model reduction method for nonlinear problems, we will keep this discussion brief and refer the interested reader to [11], [16].

Given a trajectory (or snapshots) of (1)

$$\mathcal{S} = \{ z(t,\cdot) \in \mathcal{H} \mid t \in [0, t_f] \}. \tag{8}$$

The spatial autocorrelation function K is defined as $K(x,\bar{x}) = \frac{1}{t_f}\int_0^{t_f} z(t,x)z^*(t,\bar{x})\ dt$, and is well defined since $z(t,x)$ is in $L^2([0,t_f];\mathcal{H})$. The function K is used as the kernel of the Fredholm problem $\int_\Omega K(x,\bar{x})\phi(\bar{x})\ d\bar{x} = \lambda\phi(x)$. Using Fredholm theory, there exist solution pairs $\{(\lambda_i,\phi_i)\}_{i=1}^\infty$, where the *POD eigenvalues* $\{\lambda_i\}_{i=1}^\infty$ satisfy $\lambda_1 \geq \lambda_2 \geq \cdots \geq 0$ with the only accumulation point at 0, and the *POD basis functions* $\{\phi_i\}_{i=1}^\infty$ are orthonormal functions, $\langle\phi_i,\phi_j\rangle_{\mathcal{H}} = \delta_{ij}$. We now consider the reduced basis of the first r terms based on a desired projection error (4): $\hat{\mathcal{H}}_r = \text{span}\{\phi_1(\cdot),\phi_2(\cdot),\cdots,\phi_r(\cdot)\}$, and approximate solutions to (1) in $\hat{\mathcal{H}}_r$ using

$$z_r^{pod}(t,\cdot) = \sum_{i=1}^{r} q_i(t)\phi_i(\cdot)\ \in \hat{\mathcal{H}}_r, \tag{9}$$

where $q_i,\ i=1,...,r$ are the POD projection coefficients.

We then define the (orthogonal) projection operator $\mathcal{T}_{\text{POD}} : \mathcal{H} \to \hat{\mathcal{H}}_r$ as follows

$$\left[\mathcal{T}_{\text{POD}} z\right](\cdot) = \sum_{i=1}^{r} \phi_i(\cdot)\langle\phi_i, z\rangle_{\mathcal{H}}. \tag{10}$$

The pseudo-inverse of $\mathcal{T}$ is the injection of $\hat{\mathcal{H}}_r$ into $\mathcal{H}$. Thus $\mathcal{T}^\dagger z = z$ for all $z \in \hat{\mathcal{H}}_r$ and since $\mathcal{T}$ is a projection operator, we have $\mathcal{T}\mathcal{T}^\dagger = \mathcal{I}_r$.

Next, we define $A_c : \hat{\mathcal{H}}_r \to \hat{\mathcal{H}}_r$ as

$$A_c = \mathcal{T}^{\dagger^*} A \mathcal{T}^\dagger. \tag{11}$$

With this selection, we can show that for any $\hat{z} \in \hat{\mathcal{H}}_r$ with $\|\hat{z}\|_{\hat{\mathcal{H}}} = 1$, the following holds: $\langle A_c\hat{z},\hat{z}\rangle = \langle A\mathcal{T}^\dagger\hat{z}, \mathcal{T}^\dagger\hat{z}\rangle \leq \max_{\|z\|_{\mathcal{H}}=1}\langle Az, z\rangle$.

Finally, to satisfy condition (D0), we define F as

$$F = (\mathcal{T}A - A_c\mathcal{T})C^\dagger, \tag{12}$$

where $C^\dagger$ is a left pseudo-inverse of the bounded linear operator C.

IV. MAIN RESULT 1: ROBUSTIFICATION OF THE OBSERVER

In this section we will use some tools from robust control theory, i.e., Lyapunov redesign techniques, e.g., [13], to robustify the nominal observer developed in the previous section.

Let us consider the case where the system (1) contains an uncertainty on h, as follows

$$\dot{z}(t) = Az(t) + Bu(t) + h(z(t),u(t)) + \Delta h(z(t)), \tag{13}$$
$$y(t) = Cz(t), \tag{14}$$

from $z(0) = z_0$, where the uncertainty $\Delta h : \mathcal{H} \to \mathcal{H}$, satisfies the following assumption.

Assumption 3: The uncertainty $\Delta h : \mathcal{H} \to \mathcal{H}$, is uniformly bounded: there exists a constant $\Delta h_{max} > 0$ such that $\|\Delta h(z)\|_{\mathcal{H}} \leq \Delta h_{max},\ \forall z \in \mathcal{H}$.

Now, if we examine the dynamics of the observer (2), we see that the observer convergence relies on the design of the nonlinear function G, in (5). To robustify the nominal design, presented in Section III, and account for the additional uncertainty term Δh, we use a Lyapunov redesign approach and add an additional term to G.

The robust observer is now written as

$$\dot{\hat{z}}(t) = A_c\hat{z}(t) + B_c u(t) + Fy(t) + G(\hat{z},u) + \Delta G(\hat{z}), \tag{15}$$

with $A_c,\ B_c,\ F,\ G$ satisfying conditions (5), (D0), (D1), (D2), and where $\Delta G : \hat{\mathcal{H}} \to \hat{\mathcal{H}}$, must be designed to compensate for any negative impact that the uncertainty Δh might have on the exponential stability of e obtained in (6).

Carrying out a similar analysis for the robust observer (15), under (5), and (D0), the associated error dynamics satisfy

$$\begin{aligned}\dot{e}(t) =& A_c e(t) + G\left(e(t) + \mathcal{T}z(t), u(t)\right) \\ & - \mathcal{T}h(z(t),u(t)) + \Delta G(\hat{z}) - \mathcal{T}\Delta h(z).\end{aligned} \tag{16}$$

In the sequel of this section, we will try to recover at least the convergence of e to a positively invariant set with a radius that we can control, regardless of the form of the bounded uncertainty Δh.

We summarize the result of this section in the following theorem.

Theorem 2: Consider the error dynamics (16) for the observer (15) and (5), tracking the uncertain system (13). Let h and Δh satisfy Assumptions 2 and 3, respectively. Define the compensation term ΔG as

$$\Delta G(\hat{z}) = k\Delta h_{max}\tilde{C}^*\tilde{C}e, \tag{17}$$

for $k < 0$, and any $\tilde{C}$ satisfying

$$\tilde{C}\mathcal{T} = C. \tag{18}$$

Then under conditions (D0), (D1), and (D2), the solution of the error dynamics equation (16) converges to the invariant set

$$S = \{e \in \hat{\mathcal{H}},\ \text{satisfying},\ k\|e\|_{\hat{\mathcal{H}}}\lambda_{min}(\tilde{C}^*\tilde{C}) + 1 \geq 0\}.$$

Proof 2: Refer to [4].

The robustification presented above guarantees asymptotic convergence of the observer. However, this robustness might lead to poor performance in practice. Thus, one is also interested in improving the transient performance of the observer. For this reason, we want to improve the robust observer presented in this section by complementing it with an active learning step. This step learns the best observer feedback gain k (in an optimal sense that we define later).

V. MAIN RESULT 2: LEARNING-BASED TUNING OF THE OBSERVER GAIN

In this section we want to merge together the robust observer given by (15), and (17), with an active learning algorithm, to improve the performance of the observer. Indeed, if we examine the results of Theorem 2, we see that the estimation error upper-bound (invariant set radius), decreases with the decrease of the negative feedback gain k. However, if we are concerned with more than asymptotic convergence to an invariant set, we need to tune the feedback gain k to achieve other performances. For instance, if one is interested in optimizing the transient behavior of the observer, the gain

k needs to be tuned to optimize a transient estimation cost performance.

To find this optimal value of the observer gain, we propose to use a data-driven optimization algorithm to *auto-tune the gain online*, while the observer is estimating the system states. This problem is strongly related to iterative feedback tuning (IFT), e.g.,[10], [3], [15]. We will follow [15], [3], and use an extremum seeking (ES)-based auto tuning approach.

We first write the feedback gain as

$$k = k_{nominal} + \delta k,\ k_{nominal} < 0, \tag{19}$$

where $k_{nominal}$ represents the nominal value of the observer gain, and δk is the necessary adjustment of the gain to improve the transient performance of the observer.

We then define the learning cost function

$$\begin{aligned} &Q(\delta k) = \textstyle\int_0^T ||e_y||^2_{\hat{\mathcal{H}}} dt,\\ &e_y(\delta k) = \hat{y}(t;\delta k) - y(t),\\ &\hat{y} = C\hat{z}, \end{aligned} \tag{20}$$

where $T > 0$, $\hat{z}$ is solution of the observer (15), (17), and y is the measured output. Furthermore, for analysis purposes, we will need the following assumptions on Q.

Assumption 4: The cost function $Q(\delta k)$ in (20) has a local minimum at $\delta k = \delta k_*$.

We propose to use the following time-varying amplitude-based ES algorithm, introduced in [20], to tune δk

$$\begin{aligned} \dot{x}_k &= -\delta_k \omega_k \sin(\omega_k t) Q(\delta k),\\ \delta k(t) &= x_k(t) + a_k \sin(\omega_k t),\\ \dot{a}_k &= -\delta_k \omega_k \epsilon_k a_k, \end{aligned} \tag{21}$$

where $\delta_k > 0,\ \omega_k > 0,\ \epsilon_k > 0$.

We can summarize the gain auto-tuning algorithm in the following Theorem.

Theorem 3: Consider the observer (5), (15), and (17), where the gain k is tuned iteratively, with each iteration being of finite time T, such that the state is reset over the tuning iteration $j = 1, 2, ...$, as $\hat{z}(jT) = \hat{z}_0,\ j = \{1, 2, ...\}$, and the gain–over iterations–is defined as

$$\begin{aligned} &k(t) = k_{nominal} + \Delta k(t),\ \ k_{nominal} > 0\\ &\Delta k(t) = \delta k((j-1)T),\ (j-1)T \le t < jT,\ j = 1, 2, 3... \end{aligned} \tag{22}$$

where δk is defined by the forward first order Euler discretization of (20), (21), with a time step equal to T. Then, the impulsive dynamic (15), (17), (20), (21), and (22), is well posed, the state vector $\hat{z}$ is uniformly bounded, and under Assumption 4, the gain k converges to a neighborhood of its local optimum value $k_{nom} + \delta k_*$.

Proof 3: Refer to [4].

VI. MAIN RESULT 3: APPLICATION TO ESTIMATION OF FLOW PROBLEMS–THE 2D BOUSSINESQ EQUATION

We consider estimating solutions to the challenging 2D Boussinesq equation. We focus on the dynamics of the velocity field $\boldsymbol{v}(x,t) : \Omega \times \mathbb{R}^+ \to \mathbb{R}^3$ and the temperature profile $T(x,t) : \Omega \times \mathbb{R}^+ \to \mathbb{R}$, where x denotes the spatial coordinate $x \in \Omega$, and $t \ge 0$ denotes the time. The spatial domain Ω considered here is a two dimensional space. The governing equations are described by Navier-Stokes equation with the condition of incompressible flow and the conservation of the energy through the heat transfer, which leads to the following coupled system

$$\rho\left(\frac{\partial \boldsymbol{v}}{\partial t} + \boldsymbol{v}\cdot\nabla\boldsymbol{v}\right) = -\nabla p + \nabla\cdot\tau(\boldsymbol{v}) + \rho\boldsymbol{g}, \tag{23}$$

$$\nabla\cdot\boldsymbol{v} = 0, \tag{24}$$

$$\rho c_p\left(\frac{\partial T}{\partial t} + \boldsymbol{v}\cdot\nabla T\right) = \nabla\left(\kappa\nabla T\right) \tag{25}$$

where ρ is the density profile, p is the pressure field, $\tau(\boldsymbol{v})$ is the viscous stress, c_p is the constant heat capacity, κ is the constant thermal conductivity, and $\boldsymbol{g} = -g\boldsymbol{e}_3$ is the gravitational force. In Boussinesq approximation, the buoyancy force is driven by changes in density $\rho = \rho_0 + \Delta\rho$ from the nominal density ρ_0, and the density change is modeled as perturbations from the nominal temperature T_0 using the perfect gas law $\Delta\rho\boldsymbol{g} = -\rho_0\beta(T - T_0)\boldsymbol{g}$, $\beta = 1/T_0$, and the constant term $\rho_0\boldsymbol{g}$ is absorbed into the pressure. The viscous stress is governed by $\tau(\boldsymbol{v}) = \rho\nu(\nabla\boldsymbol{v} + \nabla\boldsymbol{v}^T)$ with kinematic viscosity ν. By introducing a characteristic length L, characteristic velocity $\boldsymbol{v}_0$, wall temperature T_w, we define the following normalized states

$$\tilde{x} = \frac{x}{L},\quad \tilde{t} = \frac{t\boldsymbol{v}_0}{L},\quad \tilde{v} = \frac{v}{v_0}, \tilde{p} = \frac{p}{\rho v_0^2},\quad \tilde{T} = \frac{T - T_0}{T_w - T_0} \tag{26}$$

Using these variables, PDEs (23)–(25) can be reduced to the following (we dropped the tilde notation)

$$\frac{\partial \boldsymbol{v}}{\partial t} + \boldsymbol{v}\cdot\nabla\boldsymbol{v} = -\nabla p + \nabla\cdot\tau(\boldsymbol{v}) + \frac{\mathrm{Gr}}{\mathrm{Re}^2}T\boldsymbol{e}_3, \tag{27}$$

$$\nabla\cdot\boldsymbol{v} = 0, \tag{28}$$

$$\frac{\partial T}{\partial t} + \boldsymbol{v}\cdot\nabla T = \nabla\left(\frac{1}{\mathrm{RePr}}\nabla T\right) \tag{29}$$

where we defined Reynolds number Re$= \frac{v_0 L}{\nu}$, Grashof number Gr$= \frac{g\beta(T_w - T_0)L^3}{\nu^2}$, and Prandtl number Pr$= \frac{\nu}{k/\rho_0 c_p}$. [1] These equations are of the form (1), where $z = (v, T)^T$, the A operator is defined by $Az = (\nabla\cdot\tau(\boldsymbol{v}), \nabla\left(\frac{1}{\mathrm{RePr}}\nabla T\right))^T$, $h(z,u) = (-\boldsymbol{v}\cdot\nabla\boldsymbol{v} + \frac{\mathrm{Gr}}{\mathrm{Re}^2}T\boldsymbol{e}_3, -\boldsymbol{v}\cdot\nabla T)^T$, and $B = 0$. We selected the case with the Reynolds number $Re = 8800$, which corresponds to a challenging near-turbulent flow. A finite element discretization of Az, and h is obtained using $n = 1579779$ elements. We consider $p = 20$ measurements of the form

$$y(t) = \left(\int_{\Omega_1} z(t,x)dx, ..., \int_{\Omega_p} z(t,x)dx\right)^T =: Cz(t) \tag{30}$$

---

[1] We are well aware that Assumption 1 does not hold in the case of the Boussinesq equations, however, we wanted to report here, and discuss with our colleagues at the conference, the encouraging results obtained applying this algorithm to a challenging thermal-fluid model. Academic examples that satisfy the local Lipschitz assumption will be presented in the journal version of this work.

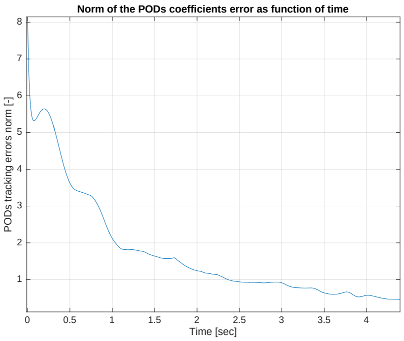

Fig. 1. Evolution of the Euclidian norm of the error between the all the estimated projected states and the true projected states.

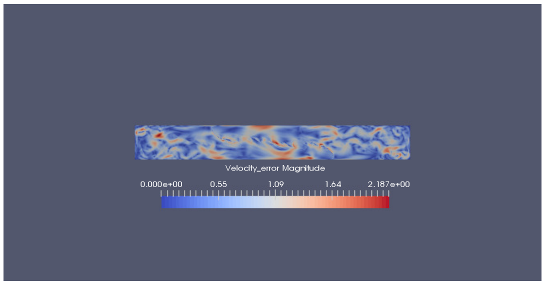

Fig. 2. Error between the estimated and the true velocity snapshot at $t = 1$ $[sec]$.

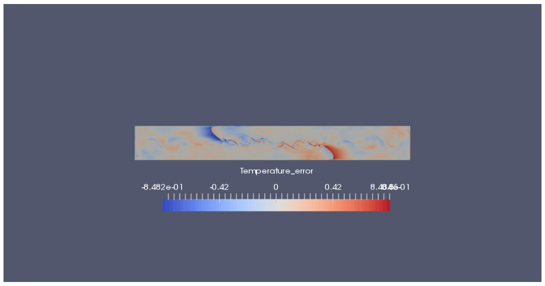

Fig. 3. Error between the estimated and the true temperature snapshot at $t = 1$ $[sec]$.

Next, the nominal observer (2) is designed using a projection with 10 POD basis functions for the velocity and 10 basis functions for the temperature. Then, A_c is obtained by projecting A onto this POD basis, which also define the projection operator $\mathcal{T}$. To check if A_c is stable, we computed the eigenvalues of A_c which are found to be all real and negative (bounded above by $-8.31e-4$).Then, F is obtained by solving equation (D0). Note that due to the high dimension of the discretized state z, the matrix C is in $\mathbb{R}^{20\times 1579779}$, which makes solving for F challenging, i.e., the pseudo-inverse in (12) induces some numerical errors that the robust observer will have to compensate for. Next, we implement the robust observer (15), (17), with $\Delta h_{max} = 1$, $k = -10^3$, and $\tilde{C} = C\mathcal{T}^{\dagger}$. To test the convergence of the estimator, we start the estimator with large initial conditions errors, s.t., $e_v(0) = 2 + v_{true}(0)$, $e_T(0) = 4T_{true}(0)$, where $e_v(0)$, $e_T(0)$ denote the initial error on the velocity, and temperature, respectively. $v_{true}(0)$, $T_{true}(0)$ denote the actual velocity and temperature, respectively. Twenty sensors that record the average temperature and sum of the velocity component averages were taken at ten unique locations for each quantity and selected using the Q-DEIM algorithm [6]. In particular, this algorithm was used to find point locations that best distinguish the ten temperature POD modes and ten velocity POD modes. The size of the integration intervals Ω_i, $i = 1, ..., p$ was selected as 0.03×0.03. Finally, To make the tests more realistic, we also added a random additive measurement noise of maximum amplitude 10^{-3}, corresponding to 38% of the maximum output measurement signal amplitude. The Euclidian norm of the error vector between all the projection states is reported in Figure 1. We can see from this plot that the estimated states converge to the true states, despite a large initial estimation error, see the rapid decay of the error vector norm in Figure 1. Some residual errors remain though, due to the measurement noise and to the numerical errors occurring when inverting the large matrices obtained from discretizing the challenging Boussinesq equations. Next, to have a better visualization of the estimation performance, we show in Figure 2, a snapshot at $t = 1$ $[sec]$ of the error between the velocity field estimate, and the true velocity. Similar snapshots are reported in Figure 3, for the temperature. It is clear from these snapshots that the initial estimates of velocity and temperature are not very precise, which is due to the introduced large initial estimation errors we imposed. To depict the estimator convergence performance, we then report in Figures 4, and 5, the velocity and temperature estimation error snapshots at $t = 4$ $[sec]$. We can see a clear estimation amelioration on both velocity and temperature fields.

To end this section, we report some numerical results on the observer's feedback gain auto-tuning. In the results reported above, we have chosen $k = -10^3$, which satisfies the basic constraint $k < 0$, as stated in Theorem 2. However, as discussed in Section V, this gain could be fine-tuned to improve the estimation performance, depending on the choice of a performance cost function. To test if we could indeed find a better gain, which implies a decrease in the learning cost (20), we implemented the auto-tuning algorithm (20, (21), with $T = 7$ $[sec]$, $\delta_k = 0.02$, $\omega =$

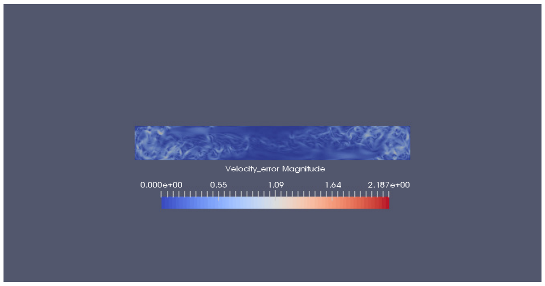

Fig. 4. Error between the estimated and the true velocity snapshot at $t = 4$ $[sec]$.

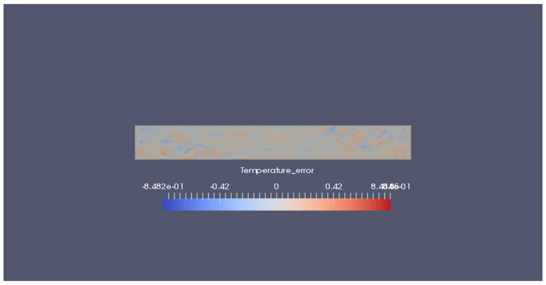

Fig. 5. Error between the estimated and the true temperature snapshot at $t = 4$ $[sec]$.

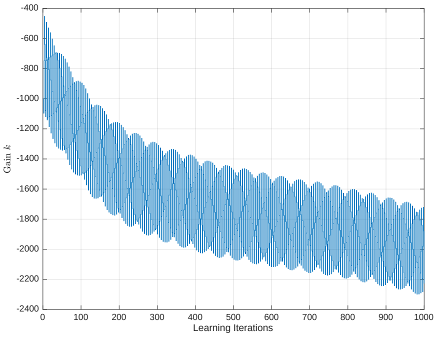

Fig. 6. Learning cost vs. number of learning iterations.

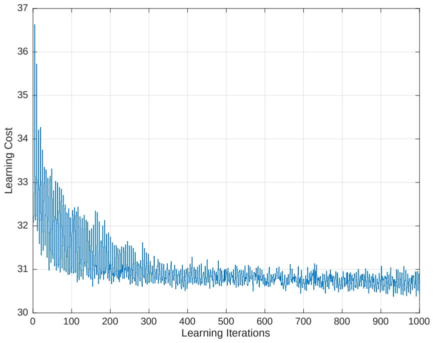

Fig. 7. Gains vs. number of learning iterations.

100 $[rad/sec]$, $\epsilon_k = 10^{-3}$, and $a_k(0) = 100$. The auto-tuning results are reported in Figures 6, 7. We can see from these figures that the learning cost in minimized, and that after 1000 iterations, we can stop the learning and select any gain from the interval $[-2200, -1800]$, which will imply a better estimation performance than the initial gain. We recall that if we keep the learning going beyond 1000 iterations, the learning amplitude a_k will eventually vanish, due to its exponential decrease as in (21), which will refine the selection to a tighter interval of gains. However, here we stoped the learning process at 1000 iterations, since we can already see the convergence trend of the learning cost function.

VII. CONCLUSIONS

The problem of robust observer design for nonlinear infinite dimension systems is challenging. The results proposed in this paper are: 1) a robust reduced order observer for nonlinear PDEs with bounded model uncertainties; 2) an IFT approach for online tuning of the observer gain; 3) an application to a challenging thermal-fluid model, namely the 2D Boussinesq equations.

Further studies will concern the case of 3D Boussinesq equations.

REFERENCES

[1] J. A. Atwell, J. Borggaard, and B. B. King. Reduced order controllers for Burgers' equation with a nonlinear observer. *International Journal of Applied Mathematics and Computer Science*, 11(6):1311–1330, 2001.

[2] M. J. Balas. Nonlinear state estimation and feedback control of nonlinear and bilinear distributed parameter systems. *Transactions of the ASME*, 102:78–82, June 1981.

[3] M. Benosman. Multi-parametric extremum seeking-based auto-tuning for robust input-output linearization control. *Int. Journal of Robust and Nonlinear Control*, 26(18):4035–4055, 2016.

[4] M. Benosman and J. Borggaard. Robust nonlinear state estimation for a class of infinite-dimensional systems using reduced-order models. *Int. Journal of Control*, 2019.

[5] J. Borggaard, S. Gugercin, and L. Zietsman. Compensators via H_2-based model reduction and proper orthogonal decomposition. In *19 th IFAC World Congress*, pages 7779–7784, South Africa, Cape Town, 2014.

[6] Z. Drmac and S. Gugercin. A new selection operator for the discrete empirical interpolation method—improved a priori error bound and extensions. *Methods and Algorithms for Scientific Computing*, 32(8):631–648, 2016.

[7] H. Feng and B.-Z. Guo. New unknown input observer and output feedback stabilization for uncertain heat equation. *Automatica*, 86:1–10, 2017.

[8] M. Guay and N. Hariharan. Airflow velocity estimation in building systems. In *IEEE American Control Conference*, pages 908–913, 2009.

[9] W. M. Haddad, V. Chellaboind, and S. G. Nersesov. *Impulsive and Hybrid Dynamical Systems: Stability, Dissipativity, and Control*. Princeton University Press, Princeton, 2006.

[10] H. Hjalmarsson. Iterative feedback tuning-an overview. *International Journal of Adaptive Control and Signal Processing*, 16(5):373–395, 2002.

[11] P. Holmes, J. L. Lumley, and G. Berkooz. *Turbulence, coherent structures, dynamical systems and symmetry*. Cambridge university press, 1998.

[12] T. John, M. Guay, N. Hariharan, and S. Narayanan. POD-based observer for estimation in Navier–Stokes flow. *Computers & Chemical Engineering*, 34(6):965–975, 2010.

[13] H. K. Khalil. *Nonlinear systems*. New York Macmillan, second edition, 1996.

[14] T. Kharkovskaya, D. Efimov, A. Polyakov, and J.-P. Richard. Design of interval observers and controls for PDEs using finite-element approximations. *Automatica*, 93:302–310, 2018.

[15] N. J. Killingsworth and M. Krstic. PID tuning using extremum seeking. *IEEE Control Systems Magazine*, pages 1429–1439, 2006.

[16] K. Kunisch and S. Volkwein. Galerkin proper orthogonal decomposition methods for a general equation in fluid dynamics. *SIAM Journal on Numerical Analysis*, 40(2):492–515, 2007.

[17] R. Miranda, J. A. Moreno, J. Chairez, and L. Fridman. Observer design for a class of hyperbolic PDE equation based on a distributed super twisting algorithm. In *12th IEEE Workshop on Variable Structure Systems*, pages 367–372, January 2012.

[18] A. Schaum, J. A. Moreno, and T. Meurer. Dissipativity-based observer design for a class of coupled 1-D semi-linear parabolic PDE systems. In *20th IFAC World Congress*, pages 98–103, Toulouse, France, 2016.

[19] A. Smyshlyaev and M. Krstic. *Adaptive Control of Parabolic PDEs*. Princeton University Press, 2010.

[20] Y. Tan, D. Nesic, I. Mareels, and A. Astolfi. On global extremum seeking in the presence of local extrema. *Automatica*, (45):245–251, 2009.

[21] M. Reyhanoglu W. MacKunis, S. V. Drakunov and L. Ukeiley. Nonlinear estimation of fluid flow velocity fields. In *IEEE Conference on Decision and Control*, pages 6931–6935, 2011.